

КРАТКИЕ СООБЩЕНИЯ

UDC 541.6:541.49:546.72:546.22

SPIN-FORBIDDEN CO BINDING TO IRON—SULFUR CLUSTER-FREE HYDROGENASE:
A DENSITY FUNCTIONAL STUDY

G.-J. Zha

School of New Energy Science and Engineering, Xinyu University, Xinyu, P. R. China
E-mail: zhaguojun_8@163.com

Received February, 7, 2016

Spin-forbidden CO binding to the iron—sulfur cluster-free hydrogenase (Hmd) is studied by the DFT calculation. The result shows that the surface of the triplet causes a PHmd—CO minimum and that ^{3,5}MECP is the lowest energy path to PHmd—CO. It is found that this CO binding involves a low barrier of 0.931 kcal/mol because of the need to change from a bound triplet state to the Hmd quintet ground state.

DOI: 10.15372/JSC20170216

Key words: density functional theory, PHmd—CO, cluster-free hydrogenase.

Hydrogenase is an enzyme that catalyzes the reversible oxidation of molecular hydrogen [1]. Its structure and catalytic mechanism are of considerable interest as a model of a highly efficient catalyst for hydrogen-fueled processes [2]. Although much effort has been devoted, the understanding of hydrogenase reactions with H₂ is still at an early stage.

One of the important hydrogenases is the [Fe]-hydrogenase, which was formerly called the iron—sulfur cluster-free hydrogenase (Hmd) [3]. In Hmd, an iron center is a catalytically active constituent of an iron guanylylpyridinol cofactor, which can be extracted from the [Fe]-hydrogenase by denaturation in the presence of mercaptoethanol [4]. Infrared spectroscopic data have revealed two CO molecules as iron ligands [5]. The X-ray absorption analysis suggested that two CO molecules, one sulfur, and one or two N/O ligands coordinated with iron [6]. Mössbauer spectroscopic data showed that iron was in a low-spin, low-oxidation state [7].

The binding and dissociation reactions of small ligands such as H₂, CO, and NO with [Fe]-hydrogenase proteins play an important part in biological processes. There have been many experimental and theoretical studies on high-spin iron—heme systems that accept crossover carbonylation to form corresponding low-spin iron—carbonyl complexes [8]. Harvey et al. [9] investigated the intrinsic barrier to the CO geminate recombination with heme compounds by the DFT calculation. In this study, we reported the reaction mechanism of CO binding with PHmd by the DFT calculation (Fig. 1). We found that a recombination of PHmd (Fig. 1, B) with CO is a spin-forbidden reaction between single CO and quintet PHmd to produce the PHmd—CO triplet, which results in a spin-state change in the central iron atom from high-spin FeII (S = 2) to low-spin FeII (S = 1).

The spin-forbidden reaction barrier to a recombination of PHmd with CO is located by characterizing the spin-state surface crossing behavior, i.e., by finding the minimum energy crossing point (MECP) between the surfaces [10—12] with a recently developed algorithm. UB3LYP density functional calculations using the Gaussian 03 software [13] are known to be accurate for general transition metal compounds and [Fe]-hydrogenated enzymes in particular [14, 15]. We performed the full geo-

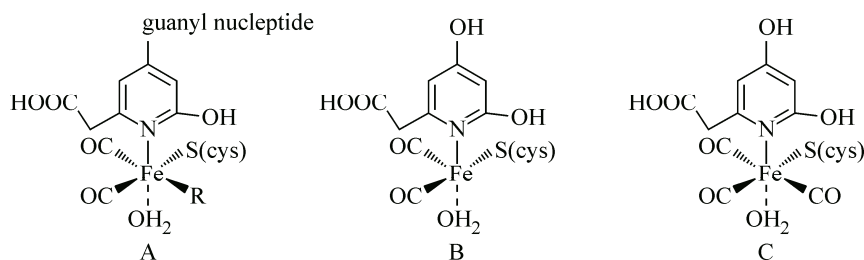


Fig. 1. Models under investigation.

A: Hmd, B: PHmd, C: PHmd-CO

metric optimization for all minimum points by assuming the C_s symmetry. We used 6-31G(*d,p*) for Fe and the Ahlrichs VTZ basis set for all other atoms.

Experimental. For PHmd coordinated with five ligands, the quintet state was calculated to be 3.215 kcal/mol and 6.213 kcal/mol more stable than the singlet and triplet states, respectively, which indicates that the quintet state is the ground state. The lengths of Fe—CO bonds in PHmd—H₂ and PHmd—COOH of 1.789 Å and 1.792 Å, respectively, are in good agreement with the experimental data [16, 17]. However, for PHmd—CO coordinated with three CO molecules with a central Fe atom, the total energy of the triplet state is -2744.28177432 a.u. lower than that of the singlet (-2744.27422082 a.u.) and quintet states (-2774.26033807 a.u.), indicating that the triplet state is the ground state. It is obvious that the coordination of third CO to Fe leads to a change in the spin state from quintet to triplet. The lengths of the three Fe—CO bonds in PHmd—CO are 1.854 Å, 1.835 Å, and 1.826 Å longer than those in PHmd—H₂ and PHmd—COOH. This result suggests that the interaction of Fe and CO in Hmd—CO is weaker than that in PHmd—H₂ and PHmd—COOH. Moreover, in PHmd and PHmd—CO complexes, the long distances between the Fe and O atoms of H₂O (3.344 Å and 3.354 Å) may be due to the Jahn—Teller distortion. This phenomenon was also found in a recent DFT geometry optimization experiment on Fe(P) without symmetry constraints [18].

Results and discussion. Fig. 1 shows that the PHmd—CO potential energy surfaces are used as a function of the reaction coordinate (roughly equivalent to the Fe—C distance, see discussion below). The triplet surface resulted in that the PHmd—CO was lowest, while the singlet and quintet spin states were exclusive. Computational results explore the reaction pathways for locating fixed points and optimal MECPs among the singlet state ^{1,5}MECP, the triplet state ^{1,3}MECP, and the quintet state ^{3,5}MECP. PHmd—CO is simulated by the FeC₁₁N₁₀O₈H₁₁S₁ model, as shown in Fig. 1, C.

The energy of three MECPs is comparable. Direct and indirect recombination pathways are ^{3,5}MECP, ^{1,5}MECP, and ^{1,3}MECP. By comparison, we found that the lowest energy PHmd—CO route is ^{3,5}MECP, although ^{1,5}MECP maintains the lowest energy. From Table 1, we see that the energy of ^{3,5}MECP is only 0.931 kcal/mol above 5A'PHmd—CO, which means that the energy barrier of the CO

T a b l e 1

Properties of PHmd-CO and MECPs stationary points

Parameter	5AH ^a	3AH ^a	1AH ^a	13E ^b	15E	35E
E_{rel} ^c	13.451	0.00	4.470	16.880	13.930	14.382
$r(\text{Fe—C})$ ^d	2.264	1.835	1.883	2.329	2.252	2.276

^a 5AH, 3AH, and 1AH present ⁵A'hmd-CO, ³A''hmd-CO and ¹A'hmd-CO.

^b 13E, 15E, and 35E present ^{1,3}MECP, ^{1,5}MECP, and ^{3,5}MECP.

^c In kcal/mol.

^d The distance between Fe and C atoms of the third CO molecule.

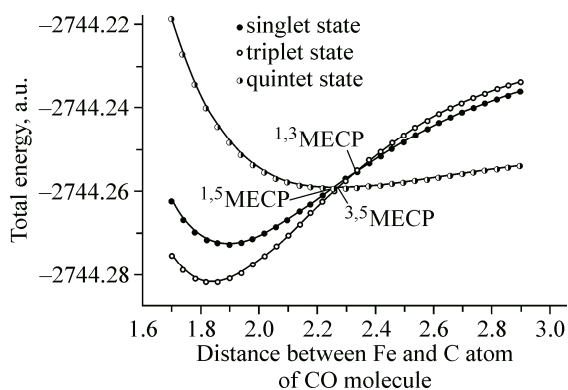


Fig. 2. Qualitative potential energy curves for heme-CO

recombination is very low. The barrier is so low that the recombination of CO with PHmd is almost a no-barrier process. In fact, Fig. 2 shows that CO will encounter almost no barriers between the bound configuration and the spin crossing, due to the triplet spin state having a strong dependence on the Fe—C bond. Harvey et al. [19] reported that the intrinsic barrier height of the CO recombination with heme compounds was about 3.0 kcal/mol, and that the energy barrier resulted from the iron atom moving

almost completely into the porphyrin plane. In the PHmd—CO system the energy barrier is very small because of immovable Fe. We found that the barrier or the transition state for the recombination of CO with PHmd had almost the same $r(\text{Fe—C})$ as the $5A'$ PHmd—CO complex (about $^{3,5}\text{MECP}$), thus there was no rejection Fe—CO interaction at $^{3,5}\text{MECP}$.

We know that the overall ligand field intensity strongly affects the spin state of an active metal site. Our DFT calculation indicates that the coordination of the third CO molecule with iron reduces the decrease in the total energy from -2744.2563 a.u. to -2744.2816 a.u. The reaction energy is about 15.9 kcal/mol. Nevertheless, for H_2 and COOH , the reaction energy is only 3.4 kcal/mol and 7.2 kcal/mol, respectively. These results indicate that the interaction of the CO molecule with Fe is much stronger than that of H_2 and COOH groups with Fe in the Hmd complex.

In order to understand the spin-forbidden reaction of CO with PHmd, an analysis of the electronic structure of PHmd—CO is necessary. The calculated ground state is also found to be a triplet state with an electronic configuration $3d(t2g)^5eg^1$. A partial contribution to the HOMO orbital is from the d_z^2 orbital of the iron atom (22.3%). The LUMO orbital of Hmd—CO represents the interaction between the d_{xy} orbital of the central iron atom and the orbital of the C atom of CO, which is composed of 26.9% of the d_{xy} orbital of the Fe atom and 34.2% of the p orbital of C atoms of the CO molecules. Obviously, it is similar to the traditional metal ligand field descriptions and the spin distribution corresponds to $(d_{xy})^2(d_{xz}, d_{yz})^3(d_z^2)^1$. The LUMO-1 orbital is composed of the π^* orbital of three CO molecules and the d_{xy} orbitals of the Fe atom. The contribution of d_{xz} is 27.3%, and the total contribution of the π^* orbitals of both CO molecules is 35.8%. The overlap of the π^* orbitals of the three CO molecules and the d_{xz} orbitals of the Fe atom is very large, which indicates that there is backbonding from the central Fe atom to the CO molecules.

It is also useful to compare the PHmd—CO UB3LYP electronic and spin ground state distributions calculated from the natural population analysis. For the Hmd—CO species, the analysis shows a d -population of 6.21 and 1.18 in the central spin density of iron ions. Both values agree with the intermediate-spin Fe(II) center and match the complex spectroscopic data. The charge in the formal d^6 excess electron configuration of the covalence population from otherwise unpopulated Fe d_{xy} and d_z^2 orbitals is due to σ -donation and backbonding from the ligand. Also, in our ^{57}Fe Mössbauer spectral calculation [20], the calculated ΔE_Q and η values of PHmd—CO are -1.247 and 0.03 mm/s, respectively, which are very close to the experimental values of -1.38 and 0.05 mm/s. The results show the importance of the rearrangement of iron and the electronic structure of the small molecule inhibitors for direct binding.

Conclusions. In this paper, we calculated the potential energy surfaces and associated energy barriers using the DFT method, which characterized spin-forbidden CO located in the model of a PHmd complex reaction barrier. We found that the CO binding involved a low barrier of 0.931 kcal/mol due to the change from the bound triplet state to the Hmd quintet ground state. The reason for this is the backbonding between the central Fe and CO molecules.

Acknowledgments. The support of the Natural Science Foundation of China (51664047) and the Foundation from the Department of Education in Jiangxi Province (GJJ161210) is gratefully acknowledged.

Supporting information includes total energies and Cartesian coordinates for all species, and orbital figure. This material is available free of charge via the Internet at <http://pubs.acs.org>.

REFERENCES

1. Vignais P.M., Billoud B., Meyer J. // Classification and phylogeny of hydrogenases, FEMS Microbiol. Rev. – 2001. – **25**. – P. 455 – 501.
2. Peters J.W., Lanzilotta W.N., Lemon B.J., Seefeldt L.C. // Science. – 1998. – **282**, N 5395. – P. 1853 – 1858.
3. Shima S., Thauer R.K. // Chem. Rec. – 2007. – **7**. – P. 37 – 46.
4. Shima S., Pilak O., Vogt S., Schick M., Stagni M.S., Meyer-Klaucke W., Warkentin E., Thauer R.K., Ermler U. // Science. – 2008. – **321**, N 5888. – P. 572 – 575.
5. Korbas M., Vogt S., Meyer-Klaucke W., Bill E., Lyon E., Thauer Rudolf Shima S.J. // Bio. Chem. – 2006. – **281**. – P. 30804 – 30813.
6. Lyon E.J., Shima S., Boecher R., Thauer R.K., Grevels F.W., Bill E., Roseboom W., Albracht S.P.J. // J. Chem. Soc. – 2004. – **126**. – P. 14239 – 14248.
7. Shima S., Lyon E.J., Thauer R.K., Mienert B., Bill E.J. // J. Am. Chem. Soc. – 2005. – **127**. – P. 10430 – 10435.
8. Steinbach P.J., Ansari A., Berendzen J., Braunstein D. // Biochemistry. – 1991. – **30**, N 16. – P. 3988 – 4001.
9. Harvey J.N., Aschi M. // J. Chem. Phys. – 1999. – **1**. – P. 5555 – 5563.
10. Maria B., José-Luis C.-M., Alexander J.C., Michael W.G., Jeremy N., Harvey P.P., Kate L.R., Xue-Zhong S., Michael T. // J. Am. Chem. Soc. – 2009. – **131**, N 10. – P. 3583 – 3592.
11. Filatov M., Shaik S. // J. Phys. Chem. A. – 1998. – **102**, N 21. – P. 3835 – 3846.
12. Carreon-Macedo J.L., Harvey J.N. // J. Am. Chem. Soc. – 2004. – **126**. – P. 5789 – 5797.
13. Frisch M.J. et al. Gaussian 03, revision C.02. – Gaussian, Inc.: Pittsburgh, PA, 2003.
14. Yang X., Hall M.B. // J. Am. Chem. Soc. – 2008. – **130**, N 43. – P. 14036 – 14037.
15. Yang X., Hall M.B. // J. Am. Chem. Soc. – 2009. – **131**. – P. 10901 – 10908.
16. Zhang Y., Mao J.H., Godbout N., Oldfield E. // J. Am. Chem. Soc. – 2000. – **124**. – P. 13921 – 13930.
17. Rovira C., Kunc K., Hutter J., Ballone P., Parrinello M. // J. Phys. Chem. A. – 1997. – **101**. – P. 8914 – 8925.
18. Zhang Y., Mao J., Oldfield E. // J. Am. Chem. Soc. – 2002. – **124**. – P. 7829 – 7839.
19. Harvey J.N. // J. Am. Chem. Soc. – 2000. – **122**, N 49. – P. 12401 – 12402.
20. Zhang Y., Oldfield E. // J. Am. Chem. Soc. – 2004. – **126**, N 14. – P. 4470 – 4471.